

# Invariant Framework for Differential Affine Signatures

**Ron Kimmel\***

Mail-stop 50A-2152, Lawrence Berkeley Laboratory,  
University of California, Berkeley, CA 94720

Email: ron@csr.lbl.gov      FAX: (510)486-5401      Tel: (510)486-5453

## Abstract

A framework for generating differential affine invariant signatures based on the gray level images of planar shapes is introduced. Non trivial invariant signatures and their corresponding arclengths are computed for planar shapes. These signatures are useful for pattern recognition and classification under partial occlusion. We deal only with implementable signatures, which practically means using up to second order derivatives, and restrict the affine transformation group accordingly. Based on the theory of affine curve evolution, an invariant gradient magnitude along the geometric scale space is defined and used as an invariant edge enhancer. The geometric heat equation for weighted (by the enhancer) affine arclength definition is shown to yield an invariant selective smoothing algorithm. This algorithm is used for image denoising in cases where we need to clean noisy images before computing invariant features. The denoising operation deforms the geometry of the object in a predictable invariant way, unlike traditional image denoising algorithms, so that the mapping between planar shapes after the denoising is preserved. The relation between the affine curvature and the Euclidean one leads to an efficient method for approximating the affine curvature signature, while the Euclidean curvature itself is used for generating the affine arclength parameter. Both curvatures are computed from the gray level image, using the implicit representation of the object's boundary as it appears in real world images. When the projection invariance assumption of the gray levels is added, robust non-trivial signatures are obtained.

*Key Words:* Object Recognition, Curve Evolution, Invariant Denoising, Invariant Signatures, Affine Transformation,.

---

\*This work was supported in part by the Applied Mathematical Science subprogram of the Office of Energy Research, U.S. Department of Energy, under Contract Number DE-AC03-76SF00098.

# 1 Introduction

An important problem in image analysis and shape understanding is the segmentation problem. The question is how to isolate an object in a given image and how to integrate object boundaries in noisy data images to achieve a good model of the object under inspection. The low level segmentation problem was addressed in many ways over the years, starting with gray level thresholding, region growing, and deformable contours based on energy minimization along a given curve called ‘snakes’. At the higher level, after an object is isolated, the problem of recognition rises. In this case the question is how to classify the given object.

Euclidean invariant operations refer to those operations for which movements and rotations of the objects in the image plane do not effect the result of the operation. We know that for pictures in the ‘real’ world, the class of transformations we encounter is much richer than pure Euclidean. In this paper we take one step into the world of transformations and deal with the affine group. The cases in which the camera is far away from the objects, so that perspective contributes minor distortions, and the objects are almost planar, may be considered (approximated) as part of the affine group. A framework that takes the affine invariance demand into consideration even before the shape is segmented, is introduced. It is shown how to deal with noisy images, and how to make use of the gray level information for generating invariant signatures and denoising algorithms.

One of the fundamental problems in pattern recognition is the problem of classifying a partially occluded object using a local description of its boundary [4, 5, 6, 7, 8, 16, 26]. On the other hand, in the field of image processing, recent non-linear geometric based algorithms were shown to give very promising results compared to ‘optimal’ linear algorithms [2, 3, 30, 32, 33]. These two research fields, that appear to be unrelated in nature, are treated in this paper by gaining the motivation from the theory of curve evolution. Specifically, we will use the affine scale space, generated by the affine heat equation as introduced in [35], to construct an affine invariant gradient magnitude. The affine gradient magnitude (affine edge enhancer) will help us in constructing an image denoising algorithm that is efficient as well as invariant to affine transformations. This algorithm is useful for denoising images before generating invariant signatures. In fact, the invariance property of the selective smoothing procedure guarantees that the change in the geometry of the shapes’ signature in the smoothed image can be predicted by applying the same algorithm to a clean reference image of the shape we try to recognize. The affine gradient magnitude will also serve as a non trivial signature for pattern classification when projection invariance of the gray levels along the shape boundary is assumed. The projection invariance of gray levels [2] states that the order of gray levels along the boundary is preserved, so that the image of the planar shape is defined as a range of gray levels and not just as interior and exterior (i.e. black and white). In other words, it is assumed that the affine transformation is operating on the gray level image. This case might be different from the case in which we first apply an affine transformation on the planar object and only then take its image. We will show how to use this gray level information along the boundary for generating simple invariant signatures.

It will be shown that the affine curvature can be approximated by a simple implementable equation exploiting the gray level information in the data image. This approximation is used for computing a simple differential affine invariant signature. A different interesting approach

for computing the affine curvature while keeping the order of derivatives low was recently introduced in [19]. It is based on the affine curvature evolution equation through the affine scale space as presented in [34].

The structure of the paper is as follows: Section 2 describes equi-affine invariant properties of planar curves, like the affine arclength, the affine normal, and the affine curvature. In Section 3 the affine heat equation as introduced in [35] is used for constructing an affine gradient magnitude and Laplacian defined along the geometric scale space. Section 4 presents an invariant selective smoothing procedure for image denoising. This procedure is shown to be equivalent to the geometric heat equation of the ‘weighted affine arclength’. In Section 5, the invariant arclength and the geometric heat equation for the linear affine arclength are presented. The knowledge about the location of one point is added to the equi-affine group yielding a subgroup of the equi-affine referred to as the ‘linear’ subgroup. Section 6 presents the intrinsic property of the weighted arclength, and an expression of the affine curvature as a function of the Euclidean curvature and its derivatives according to the Euclidean arclength. Then, Section 7 presents considerations for implementing the proposed procedures, and an approximation of the affine curvature that uses up to second order derivatives along the implicit representation of the boundary (i.e. the data image). Section 8 presents some examples of using the proposed techniques for generating efficient and robust affine invariant signatures, and of using the dynamic weighted affine geometric heat equation for image denoising. In the appendix, it is shown how to express the Euclidean curvature and its derivatives from an implicit representation of the boundary, and how to approximate the affine curvature.

## 2 Affine Invariants of Planar Curves

We shall start by introducing some basic concepts from the theory of affine differential geometry of planar curves. More details can be found in [11].

Let  $\mathcal{C}(p) : [a, b] \rightarrow \mathbb{R}^2$  be a simple regular parametric planar curve (in its planar coordinates:  $\mathcal{C}(p) = \{x(p), y(p)\}$ ). Let  $v$  be the Euclidean arclength so that<sup>1</sup>

$$v(p) = \int_0^p \langle \mathcal{C}_{\tilde{p}}, \mathcal{C}_{\tilde{p}} \rangle^{1/2} d\tilde{p},$$

where  $\tilde{p} \in [a, b]$  is an arbitrary parameterization. The tangent is known to be given by  $\mathcal{C}_v = \vec{T}$ , and the Euclidean curvature vector is given by  $\mathcal{C}_{vv} = \kappa \vec{N}$ , where  $\vec{N}$  is the curve normal and  $\kappa$  is the Euclidean curvature. We will use  $(X, Y)$  as the determinants of the  $2 \times 2$  matrix whose columns are given by the vectors  $X, Y \in \mathbb{R}^2$ . The equi-affine group is a sub-group of the affine in the sense of restricting the affine to preserve area. Given the general affine transformation  $\hat{\mathcal{C}} = \mathcal{A}\mathcal{C} + \mathbf{b}$ , the restriction is:  $\det(\mathcal{A}) = 1$ . We will consider two cases of the equi-affine transformation. The first operating on the whole image,  $I(x, y)$ , of the object:  $\hat{I}(x, y) = I(ax + by + c, dx + ey + f)$ , which will be referred to as the *gray level projection invariance assumption*. This assumption usually simplify the complexity

---

<sup>1</sup>We will use the following notations along the paper:  $\mathcal{C}_p \equiv \frac{\partial \mathcal{C}}{\partial p}$ ,  $\langle \{a, b\}, \{c, d\} \rangle \equiv ac + bd$ , and  $(\{a, b\}, \{c, d\}) \equiv ad - bc$ .

involved in generating invariant signatures. The second transformation operates only on the a boundary of the planar object, while the transformation relating the intensity at the rest of the original image to the transformed one is unknown (a more realistic assumption in most practical cases).

The equi-affine arclength  $s$  is defined so that

$$(\mathcal{C}_s, \mathcal{C}_{ss}) = 1, \quad (1)$$

and is given by [11]

$$s(p) = \int_0^p |(\mathcal{C}_{\tilde{p}}, \mathcal{C}_{\tilde{p}\tilde{p}})|^{1/3} d\tilde{p},$$

see Figure 1, which is an intrinsic integral (as we will see in Section 6).

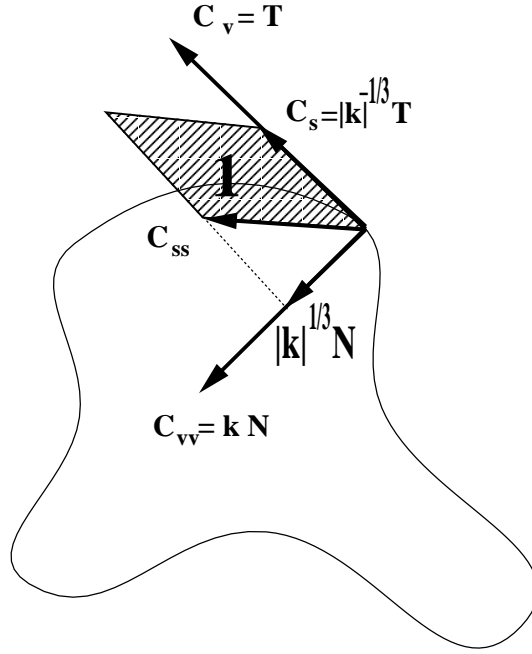


Figure 1: For  $s =$  the affine arclength and  $v =$  the Euclidean one, the relations between  $\mathcal{C}_s, \mathcal{C}_{ss}, \mathcal{C}_v$  and  $\mathcal{C}_{vv}$  are presented.

Using the intrinsic property, the relation between the Euclidean and affine arclength [36] is obtained from

$$s = \int |(\mathcal{C}_v, \mathcal{C}_{vv})|^{1/3} dv,$$

that yields

$$\begin{aligned} \frac{ds}{dv} &= |(\mathcal{C}_v, \mathcal{C}_{vv})|^{1/3} \\ &= |(\vec{T}, \kappa \vec{N})|^{1/3} \\ &= |\kappa|^{1/3}. \end{aligned} \quad (2)$$

Using the above expression, the affine tangent is given by

$$\mathcal{C}_s = \mathcal{C}_v \frac{\partial v}{\partial s} = |\kappa|^{-1/3} \vec{T}.$$

Differentiating Equation (1) we have

$$(\mathcal{C}_s, \mathcal{C}_{sss}) = 0, \tag{3}$$

which means that the vectors  $\mathcal{C}_s$  and  $\mathcal{C}_{sss}$  are linearly dependent:  $\mathcal{C}_{sss} = -\mu \mathcal{C}_s$ . The scalar  $\mu$  is the simplest affine differential invariant of the curve  $\mathcal{C}$ , known as the *affine curvature*, and  $\mathcal{C}_{ss}$  is the affine normal vector. A direct result from the last equation is

$$\mu = (\mathcal{C}_{ss}, \mathcal{C}_{sss}).$$

Differentiating Equation (3) with respect to  $s$ , it also follows that

$$\mu = (\mathcal{C}_{ssss}, \mathcal{C}_s).$$

It can be shown that  $\mu$ , the affine curvature, is the fastest normal velocity minimizing the affine arclength. However, unlike the Euclidean arclength shortening flow ( $\mathcal{C}_t = \kappa \vec{N}$ ) which is identical to the Euclidean geometric heat equation ( $\mathcal{C}_t = \mathcal{C}_{vv}$ ), it does not lead to any constructive smoothing scale space. The result of minimizing the affine arclength itself will lead to polygons, since along the straight lines the affine arclength measure is zero<sup>2</sup>. Moreover, the vertices of the polygon are also of measure zero, since as was just shown  $ds = |\kappa|^{1/3} |dv|$ . So when either the curvature or the Euclidean arclength are equal to zero, the affine arclength will be zero. One may argue that at the vertices the curvature goes to infinity. However, note that when approximating a vertex as a small circle with radius that goes to zero, it is straight forward to verify that the arclength measure is zero at the vertices:

$$\begin{aligned} \int ds &\equiv \int_{\text{vertex}} \kappa^{1/3} dv \leq \lim_{r \rightarrow 0} \left( \frac{1}{r^{1/3}} 2\pi r \right) \\ &= 2\pi \lim_{r \rightarrow 0} r^{2/3} \\ &= 0. \end{aligned}$$

This is the reason that causes direct affine arclength minimizations to fail when trying to form ‘affine snakes.’ The affine scale space [36] is achieved by the affine geometric heat equation  $\mathcal{C}_t = \mathcal{C}_{ss}$ .

In the next section, the affine gradient magnitude along the scale space [34] is used to define an invariant edge enhancer. The edge enhancer will be used for signature generation and for constructing an image invariant denoising algorithm.

---

<sup>2</sup>Basically, the affine geometry is defined for strictly convex curves in which straight lines are excluded. Nevertheless, we will use the extended definition following Sapiro and Tannenbaum [37].

### 3 Affine Edge Enhancer

For constructing an edge enhancer we will use the *affine geometric heat equation* as presented in [35]. In the proposed model all the level sets of the data image are simultaneously evolved so that each gray level set is propagating according to

$$\mathcal{C}_t = \mathcal{C}_{ss}. \quad (4)$$

Now  $\mathcal{C}(s, t) : [a, b] \times [0, T) \rightarrow \mathbb{R}^2$ , is a two parametric curve, where  $s$  is the affine arclength, and  $t$  indicates the ‘time’ of evolution. Observe that

$$\begin{aligned} \mathcal{C}_{ss} &= \frac{\partial}{\partial s} \left( \mathcal{C}_v \frac{\partial v}{\partial s} \right) \\ &= \mathcal{C}_{vv} \left( \frac{\partial v}{\partial s} \right)^2 + \mathcal{C}_v \frac{\partial^2 v}{\partial s^2} \\ &= \kappa \vec{\mathcal{N}} |\kappa^{-1/3}|^2 + \vec{\mathcal{T}} \frac{\partial^2 v}{\partial s^2} \\ &= \kappa^{1/3} \vec{\mathcal{N}} + \vec{\mathcal{T}} \frac{\partial^2 v}{\partial s^2}. \end{aligned}$$

Considering only the normal component in the evolution (the tangential component affects only the internal parameterization and does not influence the shape of the propagating curve [17]) the corresponding evolution equation is given [34] by

$$\mathcal{C}_t = \kappa^{1/3} \vec{\mathcal{N}}. \quad (5)$$

Consider the three dimensional function  $\phi(x, y, t) : \mathbb{R}^2 \times [0, T) \rightarrow \mathbb{R}$  for which each level set  $\mathcal{C} = \phi^{-1}(c)$  is evolving according to Equation (5). The implicit (Eulerian) formulation [31] of (5) (see Section 7 and the appendix) is given by:

$$\begin{aligned} \phi_t &= \left( \nabla \cdot \left( \frac{\nabla \phi}{|\nabla \phi|} \right) \right)^{1/3} |\nabla \phi| \\ &= \left( \phi_{xx} \phi_y^2 - 2\phi_x \phi_y \phi_{xy} + \phi_{yy} \phi_x^2 \right)^{1/3}. \end{aligned}$$

Given  $\phi(x, y, 0) = I(x, y)$  one can evolve the whole image according to the ‘affine geometric heat equation’ so that  $\phi(x, y, \Delta T)$  is the result of propagating  $\phi$  for  $t = \Delta T$  (see [2, 35, 38] for more details on the above equation used as an affine invariant geometric smoothing operator on images.) We shall denote by  $E(\Delta T)$  the evolution operation for  $t = \Delta T$ , i.e.  $\phi(\Delta T) \equiv E(\Delta T) \circ \phi(0)$ . Obviously  $E$  is an affine invariant operation [35], i.e.  $A \circ E(\Delta T) \circ \phi(0) = E(\Delta T) \circ A \circ \phi(0)$ , where  $A$  is the affine transformation.

Define the *affine gradient magnitude*  $G(\Delta T) \circ \phi(0) \equiv \frac{\phi(\Delta T) - \phi(0)}{\Delta T}$ . Then we readily have the following lemma

**Lemma 1** *The operation defined by  $G(\Delta T) \circ \phi(0) \equiv \frac{\phi(\Delta T) - \phi(0)}{\Delta T}$ , is invariant under the equi-affine transformation.*

*Proof.*

$$\begin{aligned}
A \circ G(\Delta T) \circ \phi(0) &= A \circ \frac{E(\Delta T) \circ \phi(0) - \phi(0)}{\Delta T} \\
&= \frac{A \circ E(\Delta T) \circ \phi(0) - A \circ \phi(0)}{\Delta T} \\
&= \frac{E(\Delta T) \circ A \circ \phi(0) - A \circ \phi(0)}{\Delta T} \\
&= G(\Delta T) \circ A \circ \phi(0).
\end{aligned}$$

■

The question is why can we consider  $|G(\Delta T) \circ I(x, y)|$ , where  $I$  is the image, to be an edge enhancer? It is obvious that edges are traversed by the evolution operation  $E(\Delta T)$  and that constant regions in the image will stay still. Yet edges of high curvature will propagate in a higher velocity than those that appear as straight lines. The curvature dependent evolution yields a non-homogeneous result along the edges when applying  $G(\Delta T)$ . The fact that at edges of high curvature the edges are enhanced may as well be considered as a desired property. For example, active contour models [14] that are used to integrate edges so as to segment object boundaries, are pushed by a geometric force that is proportional to the curvature of the propagating contour. The result of the geometric affine edge enhancer that enhances edges of high curvature therefore helps in the convergence of the active contour near the boundary, when used as the underlying potential.

In a similar way one can define the *affine Laplacian*  $\mathcal{L}(\Delta T)$  to be:

$$\mathcal{L}(\Delta T) \circ \phi(0) \equiv \frac{\phi(2\Delta T) - 2\phi(\Delta T) + \phi(0)}{\Delta T^2}.$$

In the following sections it is shown how to use the affine gradient magnitude for constructing invariant differential signatures for object recognition under partial occlusion, and image invariant denoising algorithm.

## 4 Invariant Image Denoising Procedure

Base on ideas put forward in [38], we now construct an invariant image selective smoothing algorithm. The proposed algorithm is a procedure for image denoising with invariant control on the changing geometry of the shape through the smoothing operation. The procedure is useful for denoising images before computing the invariant signatures. It can thus be considered as a step towards the calculations leading to the invariant signatures. Its relation to the total variation decreasing algorithms and to geometric heat equations are explored.

Gradient based edge detectors are usually based on the discretization of edge enhancer  $|\nabla G_\sigma * I|$ , see [13], which is equivalent to  $G_\sigma * |\nabla I|$ . The convolution with a Gaussian kernel  $G_\sigma$  is performed in order to overcome small perturbations and insignificant, high frequency, spatial noise. The variance of the smoothing operator  $\sigma$  is analog in our  $|G(\Delta T) \circ I|$  model, to  $\Delta T$  the amount of smoothing.

In [33], the authors deal with image denoising they named *nonlinear total variation based noise removal* by minimizing the integral

$$\int |\nabla I| dx dy.$$

Convergence is achieved by limiting the displacement of the result from the noisy image to be proportional to the noise variance. It is done by adding a stopping condition to prevent over smoothing, e.g.  $\int (\phi(t) - \phi(0))^2 dx dy = \sigma^2$  (for  $\phi(0) = I(x, y)$ ). We have noticed that the same results (in some cases even more efficiently, yet without the convergence property) are achieved by limiting the time of evolution in the following scheme. Where the time of evolution is now proportional to the noise variance.

The resulting minimization scheme is

$$\phi_t = \frac{\phi_x^2 \phi_{yy} - 2\phi_x \phi_y \phi_{xy} + \phi_y^2 \phi_{xx}}{(\phi_x^2 + \phi_y^2)^{3/2}} \quad \text{given} \quad \phi(0) = I(x, y),$$

according to which<sup>3</sup>, each level set of the function  $\phi$  is evolving via

$$\mathcal{C}_t = \frac{1}{|\nabla \phi|} \kappa \vec{\mathcal{N}}.$$

The last equation can be read as

$$\mathcal{C}_t = \frac{1}{\text{edge enhancer of } \phi(t)} \times \text{geometric smoothing},$$

that leads to conditional geometric smoothing or ‘selective smoothing’ according to [2], so that at regions of high gradient (close to an edge) the smoothing is low, while at constant regions the smoothing is high. It is possible to replace the  $1/|\nabla \phi|$  with more sophisticated dynamic edge enhancers which take us to other kinds of algorithms [3].

In cases where clean edges are given, yet the image itself is very noisy, it is possible to use the edges information for selecting the smoothing regions. A mask of weights is built from the initial given edges, and then used to control the smoothing process so that each level is propagating by

$$\mathcal{C}_t = W(x, y) \kappa \vec{\mathcal{N}},$$

where  $W(x, y) = \frac{1}{\text{given clean edges of } I(x, y)}$ , is the control mask.

The same motivation from the above Euclidean case direct us towards the construction of an affine invariant image denoising algorithm. Define a potential function  $f : \mathbb{R}^2 \times [0, T) \rightarrow \mathbb{R}^+$ ,

$$f(x, y, t) = F(|G(\Delta T) \circ \phi(t)|),$$

where  $F(\cdot) : \mathbb{R}^+ \rightarrow \mathbb{R}^+$  is a decreasing function. Then, the invariant denoising procedure is performed via

$$\phi_t = f(x, y, t) (\phi_x^2 \phi_{yy} - 2\phi_x \phi_y \phi_{xy} + \phi_y^2 \phi_{xx})^{1/3} \quad \text{given} \quad \phi(0) = I(x, y), \quad (6)$$

---

<sup>3</sup>One should be careful in dealing with the fact that the gradient may vanish ( $|\nabla \phi| = 0$ ). However, here we give the total variation approach only as a motivation.

according to which, each level set of the function  $\phi$  is evolving by

$$\mathcal{C}_t = f(x, y, t) \kappa^{1/3} \vec{\mathcal{N}}. \quad (7)$$

Selecting a static inverse edge enhancer function  $f(x, y, t) = f(x, y, 0) = F(|G(\Delta T) \circ \phi(0)|)$ , Equation (7) becomes exactly the geometric heat equation  $\mathcal{C}_t = \mathcal{C}_{\tilde{s}\tilde{s}}$  of the ‘weighted equi-affine arclength’:

$$d\tilde{s} = g(\mathcal{C}) |(\mathcal{C}_p, \mathcal{C}_{pp})|^{1/3} dp$$

where  $g(x, y) = 1/\sqrt{f(x, y)}$ , and since  $f$  is affine invariant,  $d\tilde{s}$  is also affine invariant. Using the causality property, the arclength may be redefined dynamically along the propagation, yielding the general invariant evolution, Equation (6).<sup>4</sup>

Taking  $\Delta T \rightarrow 0$  in the affine gradient magnitude definition, results

$$\begin{aligned} G(0) \circ \phi(0) &\equiv \lim_{\Delta T \rightarrow 0} (G(\Delta T) \circ \phi(0)) = \lim_{\Delta T \rightarrow 0} \left( \frac{\phi(\Delta T) - \phi(0)}{\Delta T} \right) \\ &= \left. \frac{d\phi(t)}{dt} \right|_{t=0} \\ &= \kappa^{1/3} |\nabla \phi(0)| \\ &= \left( \phi_x^2 \phi_{yy} - 2\phi_x \phi_y \phi_{xy} + \phi_y^2 \phi_{xx} \right)^{1/3}. \end{aligned} \quad (8)$$

A version (without the 1/3 factor) of the above operation was found to be a useful tool as an ‘edge-curvature strength’ [20] (which was obviously found to be ‘relative affine invariant’), or ‘stronger response of the curvature near edges’ [24], etc.

As an example, let  $f(x, y, t) = 1/|G(\Delta T) \circ \phi(t)|$  and  $\Delta T \rightarrow 0$ , so that  $f(x, y, t) = \frac{1}{|\kappa^{1/3} |\nabla \phi(t)|}$ . Then Equation (6) becomes

$$\phi_t = \text{sign}(\kappa),$$

and each level set of  $\phi$  is propagating via

$$\mathcal{C}_t = \frac{\text{sign}(\kappa)}{|\nabla \phi|} \vec{\mathcal{N}},$$

which is a conditional offsetting procedure. Although affine invariant as well as conditionally ‘variation decreasing’, the above evolution is unstable near inflection points, and tends to form shocks. Selecting  $\Delta T > 0$  results a smoothed version of the above example.

To summarize, using the geometric heat equation that is based on the right arclength, we have constructed an affine invariant noise removal algorithm. The algorithm is invariant in the sense that the result of the algorithm when applied to a given image is transferred exactly to the result of applying the algorithm to the transformed image. It is useful for cleaning noisy images with the ability to predict the geometry deformation that is caused by the smoothing process.

---

<sup>4</sup>Such an affine invariant evolution of all the gray level sets simultaneously is invariant under the ‘projection invariance’ assumption as presented in [2].

In [8] the arclength and curvature for the projective and its general subgroups were introduced. In the following section, simple arclength for the linear affine group are used to define the corresponding heat equation. Here, we add one point to the affine group. In practice, we deal with shape descriptors in which there exist one anchor point to simplify the arclength definition. This arclength is referred to as semi-differential invariant in [6, 26]. By ‘simple arclength’ we refer to an invariant arclength that is defined by, at most, second order derivatives of the curve.

## 5 Linear-Equi-Affine Arclength and Evolution

In [10, 27] the authors argue that Equation (4), leads towards the *geometric heat evolution equation* of any given metric which is given by

$$\mathcal{C}_t = \mathcal{C}_{rr},$$

where  $r$  is the arclength defined for the specific transformation group. Simulating these evolution equations it is enough to track only the normal component of the evolution velocity, so that geometrically the above equation may be written as<sup>5</sup>

$$\mathcal{C}_t = \langle \mathcal{C}_{rr}, \vec{\mathcal{N}} \rangle \vec{\mathcal{N}}.$$

This way it is possible [34] to reformulate the affine heat equation  $\mathcal{C}_t = \mathcal{C}_{ss}$  into its geometric equivalent  $\mathcal{C}_t = \kappa^{1/3} \vec{\mathcal{N}}$ . In [27] it was also shown that for the similarity group the inverse geometric heat equation, given by

$$\mathcal{C}_t = -\frac{1}{\kappa} \vec{\mathcal{N}},$$

is invariant. Yet it can be applied only to convex shapes.

In this section we introduce an invariant evolution of the affine group with one given point (e.g. given origin, or any other point). Using the same argument as for the equi-affine arclength, that is areas are invariant under the affine transformation, let the linear affine arclength be given by [6, 26]

$$w = \int |(\mathcal{C}, \mathcal{C}_p)| dp.$$

See Figure 2. As may be easily verified (following the same steps as the proof of Lemma 2 in the following section) this is an intrinsic measure that does not depend on the parameter, and therefore equivalent to

$$w = \int |(\mathcal{C}, \vec{T})| dv,$$

where  $v$  is the Euclidean arclength as before.

---

<sup>5</sup>The Eulerian formulation of  $\mathcal{C}_t = \langle \mathcal{C}_{rr}, \vec{\mathcal{N}} \rangle \vec{\mathcal{N}}$  is  $\phi_t = \langle \mathcal{C}_{rr}, \nabla \phi \rangle$ , see Section 7.

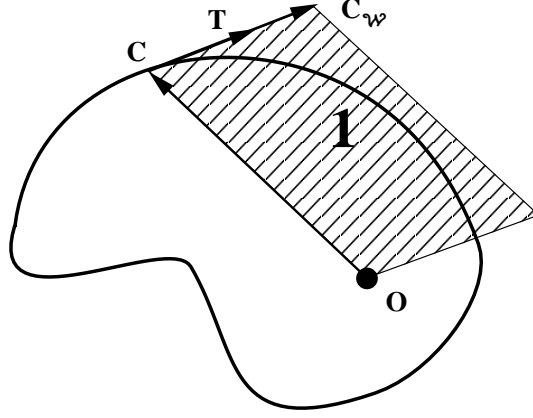


Figure 2: For  $w =$  linear affine arclength, the area  $|\langle \mathcal{C}, \mathcal{C}_w \rangle| \equiv 1$ .

The area of a closed shape [21] is given by

$$\begin{aligned} \mathcal{A} &= \frac{1}{2} \oint \langle \mathcal{C}, \vec{T} \rangle dv \\ &= \frac{1}{2} \oint \langle \mathcal{C}, \vec{\mathcal{N}} \rangle dv. \end{aligned}$$

Therefore, the arclength (as for the equi-affine one) corresponds to an area, and thus invariant. An arclength element is given by

$$\begin{aligned} dw &= |\langle \mathcal{C}, \vec{T} \rangle| dv \\ &= |\langle \mathcal{C}, \vec{\mathcal{N}} \rangle| dv. \end{aligned}$$

Thus,

$$\mathcal{C}_w = \mathcal{C}_v \frac{\partial v}{\partial s} = \mathcal{C}_v \frac{1}{|\langle \mathcal{C}, \vec{\mathcal{N}} \rangle|} = \frac{1}{|\langle \mathcal{C}, \vec{\mathcal{N}} \rangle|} \vec{T},$$

and

$$\begin{aligned} \mathcal{C}_{ww} &= \mathcal{C}_{vv} \left( \frac{\partial v}{\partial w} \right)^2 + \mathcal{C}_v \frac{\partial^2 v}{\partial w^2} \\ &= \kappa \vec{\mathcal{N}} \left( \frac{1}{|\langle \mathcal{C}, \vec{\mathcal{N}} \rangle|} \right)^2 + \frac{\partial^2 v}{\partial w^2} \vec{T} \\ &= \frac{1}{\langle \mathcal{C}, \vec{\mathcal{N}} \rangle^2} \kappa \vec{\mathcal{N}} + \text{tangential component}. \end{aligned}$$

The corresponding linear affine heat equation given by its geometric Euclidean version is

$$\mathcal{C}_t = \frac{1}{\langle \mathcal{C}, \vec{\mathcal{N}} \rangle^2} \kappa \vec{\mathcal{N}}. \quad (9)$$

Observe that when considering closed curves, the interesting cases are those in which the anchor point is located inside the curve and no tangent points are formed. In other cases, it is possible to locate the smallest triangle that is formed by two tangent points (it is easy to prove that there exist at least two) and the anchor point. This triangle is then mapped into a given reference triangle for every data image, and the same mapping is used to eliminate the transformation effect, see Figure 3. So, considering only the ‘interesting’ cases, the geometric heat equation (9) is not influenced by singular values since tangent points are excluded. Equation (9) is given here as an example for using the second derivative according to the invariant arclength. It is not claimed here to perform better than the affine heat equation. However, observe that the embedding property is preserved under this flow by the fact that when two embedded curves touch at a point, their normals coincide, and the curvature flow (normalized by a constant) takes over.

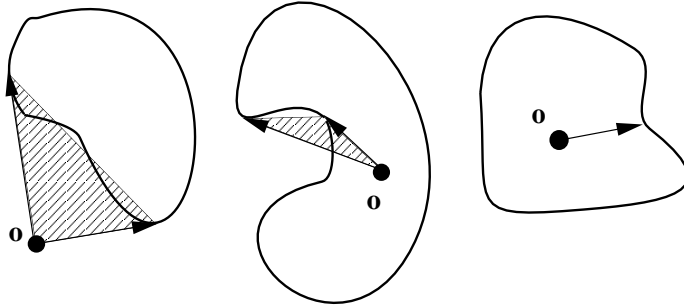


Figure 3: There are three possible locations for the given point: Outside the shape, in which  $\mathcal{C}(p)$  is tangent at least twice to the boundary of the shape. Inside a shape which consists of a concave part that leads again to at least two tangent points. Inside a shape with no tangents at all, which is the interesting case from our point of view.

## 6 Arclength Definition and Intrinsic Functionals

In this section, we show that by ‘weighing’ the affine arclength, the intrinsic property of the arclength does not break. Then, the relation between the affine curvature and the Euclidean one is used to generate a simple non trivial differential shape descriptor. We refer to such as *affine invariant signatures*.

Define a ‘non-edge’ penalty function  $g : \mathbb{R}^2 \rightarrow \mathbb{R}^+$ ,  $g(x, y) = F(G(\Delta T) \circ I(x, y))$  that  $F$  being a one to one mapping makes  $g$  also affine invariant. For example, let

$$g(x, y) = \frac{1}{|G(\Delta T) \circ I(x, y)|}. \quad (10)$$

The function  $g$  maps edges to low positive values and constant regions to high positive values. Actually any decreasing positive function  $g$  of an affine gradient magnitude is valid for the rest of our discussion.

Without breaking the invariance property, we integrate  $g$  along the affine arclength. Let

$$L(\mathcal{C}, \mathcal{C}_p, \mathcal{C}_{pp}) = g(\mathcal{C}(p))(\mathcal{C}_p, \mathcal{C}_{pp})^{1/3}.$$

We will consider the following functional as the ‘weighted affine arclength’

$$S[\mathcal{C}] = \int L(\mathcal{C}, \mathcal{C}_p, \mathcal{C}_{pp}) dp. \quad (11)$$

Let us prove that (11) is free of parameterization [22] (i.e. an intrinsic integral). We note that this is only an example, and the intrinsic property should hold for any arclength.

**Lemma 2** *The functional*

$$\int_{p_0}^{p_1} g(\mathcal{C}(p))(\mathcal{C}_p, \mathcal{C}_{pp})^{1/3} dp$$

*depends only on the curve in the  $xy$ -plane<sup>6</sup> defined by the parametric equation  $x = x(p)$ ,  $y = y(p)$ , and not on the choice of the parametric representation of the curve.*

*Proof.* We show that if we go from  $p$  to a new parameter  $r$  by setting  $p = p(r)$ , where  $dp/dr > 0$  and the interval  $[p_0, p_1]$  goes into  $[r_0, r_1]$ , then

$$\int_{r_0}^{r_1} g(\mathcal{C}(r))(\mathcal{C}_r, \mathcal{C}_{rr})^{1/3} dr = \int_{p_0}^{p_1} g(\mathcal{C}(p))(\mathcal{C}_p, \mathcal{C}_{pp})^{1/3} dp.$$

Since we have  $y_r = y_p p_r$ ,  $y_{rr} = y_{pp} p_r^2 + y_p p_{rr}$  and similarly  $x_r = x_p p_r$ ,  $x_{rr} = x_{pp} p_r^2 + x_p p_{rr}$ , it follows that

$$\begin{aligned} & \int_{r_0}^{r_1} g(\mathcal{C}(r))(\mathcal{C}_r, \mathcal{C}_{rr})^{1/3} dr \\ &= \int_{r_0}^{r_1} g(\mathcal{C}(r)) \left( x_p p_r (y_{pp} p_r^2 + y_p p_{rr}) - y_p p_r (x_{pp} p_r^2 + x_p p_{rr}) \right)^{1/3} dr \\ &= \int_{r_0}^{r_1} g(\mathcal{C}(r)) \left( x_p y_{pp} p_r^3 - y_p x_{pp} p_r^3 \right)^{1/3} dr \\ &= \int_{r_0}^{r_1} g(\mathcal{C}(r)) (x_p y_{pp} - y_p x_{pp})^{1/3} \frac{dp}{dr} dr = \int_{p_0}^{p_1} g(\mathcal{C}(p))(\mathcal{C}_p, \mathcal{C}_{pp})^{1/3} dp. \end{aligned}$$

■

Lemma 2 guarantees that the functional (11) is free of the parameterization of the curve. In fact, in the general case of selecting an arclength for a given transformation group, the integral must be intrinsic! It should have the general form of  $dl = [\text{geometric quantity}] \times |\mathcal{C}_p| dp$ , where ‘geometric quantity’ is 1 for the Euclidean group,  $|k(p)|^{1/3}$  for the equi-affine group,  $|k(p)|$  for the similarity,  $|(\mathcal{C}(p), \vec{T}(p))|$  for the linear-affine, etc..

Lemma 2 can be used to find the relation between the affine curvature  $\mu$  and the curvature derivatives  $\kappa$ ,  $\kappa_v$  and  $\kappa_{vv}$ , by minimizing the affine arclength, using the resulting Euler-Lagrange equations, and the relations presented in Section 2. The same relation could be found in other ways as well [11, 26, 34].

<sup>6</sup>often referred to as the ‘orbit’, ‘trace’ or ‘image’ of the curve  $\mathcal{C}(p)$

The computation of the affine curvature  $\mu$  involves derivatives of the fourth order, and may be computed as presented in [11]. Expressing the affine curvature  $\mu$  as a function of the Euclidean curvature  $\kappa$  (see [26, 34]), yields

$$\mu = \kappa^{4/3} - \frac{5}{9}\kappa^{-8/3}\kappa_v^2 + \frac{1}{3}\kappa^{-5/3}\kappa_{vv}. \quad (12)$$

In the following section and in the appendix, we show how to approximate the affine curvature based on Equation (12), and use it to construct invariant signatures. This approximation will use up to second order derivatives of the the implicit representation of the object boundary. Which means a direct operation on the data image, before any thresholding is performed.

## 7 Implementation Considerations

Before thresholding, the object boundary is given in an implicit representation, e.g. the boundary is defined as a given gray level set of the data image:  $I(x, y) = \text{Threshold}$ , see [23]. For all of our implementations of curve evolution as well as the computation of the affine and Euclidean curvatures this implicit level set representation is used. Similarly, implicit representation of planar curves will be used for the curve evolution implementations. We refer the interested reader to the growing literature on level set motion for curve and surface evolution, starting with the Osher Sethian classical paper [31].

The basic idea is to map the ‘time’ dependent coordinates  $(p, t)$  to fixed coordinates  $(x, y, t)$  by embedding the propagating contour in a higher dimensional function. The level sets of the function  $\phi(x, y, t) : \mathbb{R}^2 \times [0, T) \rightarrow \mathbb{R}$  propagating according to

$$\phi_t = \alpha|\nabla\phi|,$$

where  $|\nabla\phi| \equiv \sqrt{\phi_x^2 + \phi_y^2}$ , are evolving according to

$$\mathcal{C}_t = \alpha\vec{\mathcal{N}}.$$

This result may be easily obtained from  $\vec{\mathcal{N}} = \{-y_v, x_v\} = \nabla\phi/|\nabla\phi|$ , and the chain rule  $\phi_t = \langle \nabla\phi, \mathcal{C}_t \rangle = \langle \nabla\phi, \alpha\vec{\mathcal{N}} \rangle = \alpha|\nabla\phi|$ .

While the embedding is preserved, as was proven for curvature based evolutions [18], there is no need to control the propagation of the higher dimensional function  $\phi$ . The embedding is preserved for morphology evolutions as well (which require additional ‘entropy condition’). However, in other cases it is needed to supervise the level sets behavior so that the zero set evolution is the dominant one, and the rest are only swept by its influence. For this purpose some numerical methods were developed like the narrow strip introduced in [1, 15], re-initialization of the function every iteration [39], expansion of the zero set velocity to the whole image domain [25], etc.

In the appendix we introduce formulas expressing  $\kappa$ ,  $\kappa_v$  and  $\kappa_{vv}$  as a function of the  $x$  and  $y$  derivatives of  $\phi$  (up to the fourth order for  $\kappa_{vv}$ ). Then to achieve practical formulas, we assume that the implicit representation along the boundary is given by polynomial patches of up to second order. This assumption holds only after affine geometric smoothing is performed

so that sharp edges are smoothed and the approximation is valid. The affine curvature as given in Equation (12) is approximated by (see Appendix A)

$$\mu \approx \tilde{\mu} = \frac{\phi_{xx}\phi_{yy} - \phi_{xy}^2}{(\phi_{xx}\phi_y^2 - 2\phi_x\phi_{xy}\phi_y + \phi_x^2\phi_{yy})^{2/3}}. \quad (13)$$

An important observation is that  $\tilde{\mu}$  is an affine invariant quantity when considering the affine transformation of the gray level image (*i.e.* under the projection invariance assumption). It is actually the ratio of the Hessian  $H = \phi_{xx}\phi_{yy} - \phi_{xy}^2$  and  $(G(0) \circ \phi)^2$  that was defined in Equation (8). Defining  $J = (G(0) \circ \phi)^3$ , it is claimed in [29] that  $H$  and  $J$  are the two basic independent affine invariant descriptors, and that all second order differential invariants are functions of  $H$  and  $J$ , see [28]

From above observation it follows that:

**Corollary 1**  $\tilde{\mu} = H/J^{2/3}$  is affine invariant under the projection invariance assumption of the gray levels, namely  $\hat{\phi}(x, y) = \phi(ax+by+c, dx+ey+f)$ , and a second order approximation of the affine curvature of the level sets of  $\phi(x, y)$ .

## 7.1 Relation to Conics

In the Euclidean case, we know that the curvature of a point along a curve is equivalent to that of the osculating circle at that point. Where the curvature of a circle is obviously a constant. In a very recent paper [12], it was noted that the affine curvature at a given point along a curve is equivalent to the affine curvature of the osculating conic to the curve at that point. Where the affine curvature of a conic is constant. The authors of [12] also presented the following theorem:

**Theorem 1** *The affine curvature of a nondegenerate conic defined implicitly by*

$$ax^2 + 2bxy + cy^2 + 2dx + 2ey + f = 0,$$

*is given as a function of two equi-affine invariants of the conic  $S$  and  $T$ , by*

$$\mu = \frac{S}{T^{2/3}},$$

where

$$S = ac - b^2 = \det \begin{vmatrix} a & b \\ c & d \end{vmatrix}, \quad T = \det \begin{vmatrix} a & b & d \\ b & c & e \\ d & e & f \end{vmatrix}.$$

The above result may be obtained directly from Corollary 1 above. While in Corollary 1 the gray level image is assumed to locally have conic level sets, Theorem 1 considers a single conic curve. *I.e.* considering the level sets  $\phi(x, y) = \text{constant}$ , with the additional assumption  $\phi(x, y) = ax^2 + 2bxy + cy^2 + 2dx + 2ey + f$ , the affine curvature of the level sets curves is given by Equation 13 which may be easily checked to be equivalent to the result of the above theorem.

## 8 Examples

The first example, Figure 4, presents the evolution of a shape according to the affine geometric heat equation  $\mathcal{C}_t = \mathcal{C}_{ss}$ , or in its implicit form (after eliminating the tangential component)  $\phi_t = (\phi_{xx}\phi_y^2 - 2\phi_x\phi_{xy}\phi_y + \phi_x^2\phi_{yy})^{1/3}$ . Next, Figure 5 demonstrates the power of the proposed framework in tracking the convex hull of objects by using the ‘weighted affine’ heat equation.

Affine invariant signatures  $\tilde{\mu}(s)$ , and  $G(\Delta T) \circ I(x, y)$  along the (smoothed) boundary

$$\mathcal{G}(s) \equiv G(\Delta T) \circ \phi(0)|_{\phi(\Delta T)=0} \quad \text{where} \quad \phi(0) = I(x, y),$$

as a function of the affine arclength, are computed by the proposed methods. It is shown in Figure 6 that the signatures of the same object under different affine transformations remain almost the same. The gradient magnitude  $\mathcal{G}(s)$  along the boundary of the smoothed object, (the zero level set of  $\phi(\Delta T)$ ) is a robust signature, yet requires the projection invariance of the gray levels. While  $\tilde{\mu}(s)$ , approximating the affine curvature, is free of any assumptions on the the gray levels in the interior and exterior of the object in the image. The signature functions are presented without any smoothing or filtering. For closed curves, Fourier descriptors of the periodic signature function may be the right choice for classification, while for recognition and classification of objects under partial occlusion, local matching methods should be applied. Another possibility is to construct a ‘signature image’ similar to the one introduced in [9]. The idea is to ‘collect’ the signatures along the scale parameter  $t$  into a family of  $\tilde{\mu}(s, t)$  or  $\mathcal{G}(s, t)$ . This results in robust signatures, however, more consuming from the matching point of view, since now the matching problem is performed in a higher dimension. Observe that the signatures of the two images are very similar, while obviously  $\kappa(v)$  is different. The affine arclength was computed by using the implicit representation of the boundary in the gray level image (see Appendix A). The Euclidean curvature at each pixel grid is interpolated at the grid intersection points with the boundary of the object. Then  $ds$  is approximated by  $\Delta s = \kappa^{1/3}\Delta v$ , where  $\Delta v$  is the length of the line connecting the zero crossings of the object boundary with a given pixel cell (a square defined by  $\{(i, j), (i, j+1), (i+1, j+1), (i+1, j)\}$ .) The Euclidean curvature is computed using its implicit representation  $\kappa = \text{div}(\nabla\phi/|\nabla\phi|)$ , and interpolated at the intersection points of the boundary and the pixel grid lines.

Denosing algorithm results are presented in Figure 7. The ‘dynamic weighted affine’ heat equation, is an affine selective smoothing operator. It is used to efficiently remove noise perturbations from the image, while preserving the edges. It is possible to predict the geometric deformation caused by this invariant selective smoothing operation, by applying the same procedure to a reference image which is an affine transformation of the data image, see Figure 8.

## 9 Concluding Remarks

In this paper the affine invariant gradient magnitude along the affine scale space was introduced and used to construct image denosing algorithms and shape invariant signature functions. The geometric heat equation of the ‘affine weighted arclength’ that integrates the affine edges and the affine arclength from ‘Affine Differential Geometry’ [11] was shown to

be an invariant selective smoothing procedure, resulting in the image denoising algorithm when the ‘dynamic affine weighted arclength’ is used.

The fourth order derivatives and the non-linear nature of the calculations of the geometrical properties, make the computation of the affine curvature signature a complicated task. We have shown that it is possible to reduce this complexity by locally approximating the implicit representation of the boundary contour as a second order polynomial function. Although such an approximation is valid only at smooth regions of the image, it is possible to treat object boundaries as such, after affine smoothing is applied to the image. Moreover, that approximation is invariant under the projection invariance assumption.

A simple differential signature was obtained directly from the affine scale space, under the projection invariance assumption. It was shown to result a robust invariant non trivial differential signatures. In most cases, the fact that the object includes non-homogeneous regions helps in making these signatures ‘more interesting’.

We conclude by a table presenting the arclength and the geometric heat equations for some of the transformation groups we dealt with. The geometric heat equations may be used for generating the invariant signatures in the same manner we did for the equi-affine group.

Group Arclength	$L(p)$	Geom. Heat Eq.
Euclidean	$\langle \mathcal{C}_p, \mathcal{C}_p \rangle^{1/2} = 1 \cdot  \mathcal{C}_p $	$\mathcal{C}_t = \kappa \vec{\mathcal{N}}$
Weighted Euclidean	$g(\mathcal{C}) \langle \mathcal{C}_p, \mathcal{C}_p \rangle^{1/2}$	$\mathcal{C}_t = \frac{\kappa}{g^2} \vec{\mathcal{N}}$
Equi-Affine	$ (\mathcal{C}_p, \mathcal{C}_{pp}) ^{1/3} =  \kappa ^{1/3}  \mathcal{C}_p $	$\mathcal{C}_t = \kappa^{1/3} \vec{\mathcal{N}}$
Weighted Affine	$g(\mathcal{C})  (\mathcal{C}_p, \mathcal{C}_{pp}) ^{1/3} = g(\mathcal{C})  \kappa ^{1/3}  \mathcal{C}_p $	$\mathcal{C}_t = \frac{1}{g^2} \kappa^{1/3} \vec{\mathcal{N}}$
Similarity	$\frac{ (\mathcal{C}_p, \mathcal{C}_{pp}) }{ \langle \mathcal{C}_p, \mathcal{C}_p \rangle } =  \kappa   \mathcal{C}_p $	$\mathcal{C}_t = \frac{1}{\kappa} \vec{\mathcal{N}}$
Linear-Equi-Affine	$ (\mathcal{C}, \mathcal{C}_p)  =  (\mathcal{C}, \vec{\mathcal{T}})   \mathcal{C}_p $	$\mathcal{C}_t = \frac{\kappa}{(\mathcal{C}, \vec{\mathcal{T}})^2} \vec{\mathcal{N}}$
Weighted Linear-Equi-Affine	$g(\mathcal{C})  (\mathcal{C}, \mathcal{C}_p)  = g(\mathcal{C})  (\mathcal{C}, \vec{\mathcal{T}})   \mathcal{C}_p $	$\mathcal{C}_t = \frac{\kappa}{g^2 (\mathcal{C}, \vec{\mathcal{T}})^2} \vec{\mathcal{N}}$
Linear Affine	$\frac{ (\mathcal{C}_p, \mathcal{C}_{pp}) }{(\mathcal{C}, \mathcal{C}_p)^2} = \frac{ \kappa }{(\mathcal{C}, \vec{\mathcal{T}})^2}  \mathcal{C}_p $ $\frac{ (\mathcal{C}, \mathcal{C}_{pp}) }{ (\mathcal{C}, \mathcal{C}_p) } = \frac{\kappa(\mathcal{C}, \vec{\mathcal{N}})}{(\mathcal{C}, \vec{\mathcal{T}})}  \mathcal{C}_p $	$\mathcal{C}_t = \frac{(\mathcal{C}, \vec{\mathcal{T}})^4}{\kappa} \vec{\mathcal{N}}$ $\mathcal{C}_t = \frac{(\mathcal{C}, \vec{\mathcal{N}})^2}{\kappa(\mathcal{C}, \vec{\mathcal{N}})^2} \vec{\mathcal{N}}$

## Acknowledgments

I would like to thank Freddy Bruckstein, Guillermo Sapiro, Doron Shaked, and Nahum Kiryati for their comments the presentation of some of the methods proposed in this report.

## Appendix A

Here the curvature  $\kappa$  of the planar curve  $\mathcal{C} = \phi^{-1}(c)$ , and its first and second derivatives ( $\kappa_v$  and  $\kappa_{vv}$ ) are computed as a function of  $\phi$ . We use the fact that along the level sets  $\mathcal{C}$  of  $\phi$ , the function does not change its values, i.e.  $\partial^n \phi / \partial v^n = 0$ , for any  $n$ . Particularly, for  $n = 2, 3, 4$ . From this, and the knowledge of the geometrical properties of  $\mathcal{C}_v, \mathcal{C}_{vv}, \mathcal{C}_{vvv}$  and  $\mathcal{C}_{vvvv}$ , we compute (using Mathematica algebraic calculations):

$$\kappa = \frac{2\phi_x \phi_{xy} \phi_y - \phi_{xx} \phi_y^2 - \phi_x^2 \phi_{yy}}{(\phi_x^2 + \phi_y^2)^{3/2}}$$

$$\begin{aligned}
\kappa_v &= (6\phi_x^3\phi_{xy}^2\phi_y - 3\phi_x^4\phi_{xyy}\phi_y + 3\phi_x^3\phi_{xxy}\phi_y^2 - 9\phi_x^2\phi_{xx}\phi_{xy}\phi_y^2 + 3\phi_x\phi_{xx}^2\phi_y^3 \\
&\quad - \phi_x^2\phi_{xxx}\phi_y^3 - 6\phi_x\phi_{xy}^2\phi_y^3 - 3\phi_x^2\phi_{xyy}\phi_y^3 + 3\phi_x\phi_{xxy}\phi_y^4 \\
&\quad + 3\phi_{xx}\phi_{xy}\phi_y^4 - \phi_{xxx}\phi_y^5 - 3\phi_x^4\phi_{xy}\phi_{yy} + 3\phi_x^3\phi_{xx}\phi_y\phi_{yy} + 9\phi_x^2\phi_{xy}\phi_y^2\phi_{yy} \\
&\quad - 3\phi_x\phi_{xx}\phi_y^3\phi_{yy} - 3\phi_x^3\phi_y\phi_y^2 + \phi_x^5\phi_{yyy} + \phi_x^3\phi_y^2\phi_{yyy})/(\phi_x^2 + \phi_y^2)^3 \\
\kappa_{vv} &= (24\phi_x^5\phi_{xy}^3\phi_y - 24\phi_x^6\phi_{xy}\phi_{xyy}\phi_y + 4\phi_x^7\phi_{xyyy}\phi_y - 6\phi_x^6\phi_{xxyy}\phi_y^2 + 36\phi_x^5\phi_{xxy}\phi_{xy}\phi_y^2 \\
&\quad - 72\phi_x^4\phi_{xx}\phi_{xy}^2\phi_y^2 + 18\phi_x^5\phi_{xx}\phi_{xyy}\phi_y^2 + 4\phi_x^5\phi_{xxy}\phi_y^3 \\
&\quad - 24\phi_x^4\phi_{xx}\phi_{xxy}\phi_y^3 + 60\phi_x^3\phi_{xx}^2\phi_{xy}\phi_y^3 - 16\phi_x^4\phi_{xxx}\phi_{xy}\phi_y^3 - 96\phi_x^3\phi_{xy}^3\phi_y^3 \\
&\quad + 12\phi_x^4\phi_{xy}\phi_{xyy}\phi_y^3 + 8\phi_x^5\phi_{xyyy}\phi_y^3 - 15\phi_x^2\phi_{xx}^3\phi_y^4 + 10\phi_x^3\phi_{xx}\phi_{xxx}\phi_y^4 - \phi_x^4\phi_{xxxx}\phi_y^4 \\
&\quad - 12\phi_x^4\phi_{xxyy}\phi_y^4 + 12\phi_x^3\phi_{xxy}\phi_{xy}\phi_y^4 + 132\phi_x^2\phi_{xx}\phi_{xy}^2\phi_y^4 + 6\phi_x^3\phi_{xx}\phi_{xyy}\phi_y^4 \\
&\quad + 8\phi_x^3\phi_{xxy}\phi_y^5 - 18\phi_x^2\phi_{xx}\phi_{xxy}\phi_y^5 - 48\phi_x\phi_{xx}^2\phi_{xy}\phi_y^5 \\
&\quad - 12\phi_x^2\phi_{xxx}\phi_{xy}\phi_y^5 + 24\phi_x\phi_{xy}^3\phi_y^5 + 36\phi_x^2\phi_{xy}\phi_{xyy}\phi_y^5 + 4\phi_x^3\phi_{xyyy}\phi_y^5 \\
&\quad + 3\phi_{xx}^3\phi_y^6 + 10\phi_x\phi_{xx}\phi_{xxx}\phi_y^6 - 2\phi_x^2\phi_{xxxx}\phi_y^6 - 6\phi_x^2\phi_{xxyy}\phi_y^6 \\
&\quad - 24\phi_x\phi_{xxy}\phi_{xy}\phi_y^6 - 12\phi_{xx}\phi_{xy}^2\phi_y^6 - 12\phi_x\phi_{xx}\phi_{xyy}\phi_y^6 + 4\phi_x\phi_{xxy}\phi_y^7 + 6\phi_{xx}\phi_{xxy}\phi_y^7 \\
&\quad + 4\phi_{xxx}\phi_{xy}\phi_y^7 - \phi_{xxx}\phi_y^8 - 12\phi_x^6\phi_{xy}^2\phi_{yy} + 6\phi_x^7\phi_{xyy}\phi_{yy} - 12\phi_x^6\phi_{xxy}\phi_y\phi_{yy} \\
&\quad + 36\phi_x^5\phi_{xx}\phi_{xy}\phi_y\phi_{yy} - 18\phi_x^4\phi_{xx}^2\phi_y^2\phi_{yy} + 6\phi_x^5\phi_{xxx}\phi_y^2\phi_{yy} + 132\phi_x^4\phi_{xy}^2\phi_y^2\phi_{yy} \\
&\quad - 18\phi_x^5\phi_{xyy}\phi_y^2\phi_{yy} + 6\phi_x^4\phi_{xxy}\phi_y^3\phi_{yy} - 144\phi_x^3\phi_{xx}\phi_{xy}\phi_y^3\phi_{yy} \\
&\quad + 33\phi_x^2\phi_{xx}^2\phi_y^4\phi_{yy} + 2\phi_x^3\phi_{xxx}\phi_y^4\phi_{yy} - 72\phi_x^2\phi_{xy}^2\phi_y^4\phi_{yy} - 24\phi_x^3\phi_{xyy}\phi_y^4\phi_{yy} \\
&\quad + 18\phi_x^2\phi_{xxy}\phi_y^5\phi_{yy} + 36\phi_x\phi_{xx}\phi_{xy}\phi_y^5\phi_{yy} - 3\phi_{xx}^2\phi_y^6\phi_{yy} - 4\phi_x\phi_{xxx}\phi_y^6\phi_{yy} \\
&\quad - 3\phi_x^6\phi_{xx}\phi_y^2 - 48\phi_x^5\phi_{xy}\phi_y\phi_y^2 + 33\phi_x^4\phi_{xx}\phi_y^2\phi_y^2 + 60\phi_x^3\phi_{xy}\phi_y^3\phi_y^2 \\
&\quad - 18\phi_x^2\phi_{xx}\phi_y^4\phi_y^2 + 3\phi_x^6\phi_{yy}^3 - 15\phi_x^4\phi_y^2\phi_{yy}^3 + 4\phi_x^7\phi_{xy}\phi_{yyy} - 4\phi_x^6\phi_{xx}\phi_y\phi_{yyy} \\
&\quad - 12\phi_x^5\phi_{xy}\phi_y^2\phi_{yyy} + 2\phi_x^4\phi_{xx}\phi_y^3\phi_{yyy} - 16\phi_x^3\phi_{xy}\phi_y^4\phi_{yyy} + 6\phi_x^2\phi_{xx}\phi_y^5\phi_{yyy} \\
&\quad + 10\phi_x^6\phi_y\phi_{yy}\phi_{yyy} + 10\phi_x^4\phi_y^3\phi_{yy}\phi_{yyy} - \phi_x^8\phi_{yyy} - 2\phi_x^6\phi_y^2\phi_{yyy} - \phi_x^4\phi_y^4\phi_{yyy})/ \\
&\quad (\phi_x^2 + \phi_y^2)^{9/2}
\end{aligned}$$

Although impressive in length, the above expressions are too long for practical implementation. Moreover, dealing with pixel based images, the large support required for the computation of the high order derivatives leads to inaccurate and noise sensitive operations around the edges.

Assuming that the implicit function  $\phi$  is smooth (can be achieved by affine smoothing) and therefore can be locally approximated by  $ax^2 + bxy + cy^2 + dx + ey + f$ . The third and fourth order derivatives of  $\phi$  may thus be neglected. Using this approximation considerably simplify the scheme, and reduces the local support to a  $3 \times 3$  pixel mask, with truncation error of  $\mathcal{O}(\Delta x^2)$  (where  $\Delta x$  is the distance between neighboring pixels).

Thereby, taking all third and fourth partial derivatives of  $\phi$  (with respect to  $x$  and  $y$ ) to be zero, the affine curvature  $\mu$  is simplified into

$$\mu = \kappa^{4/3} - \frac{5\kappa_v^2}{9\kappa^{8/3}} + \frac{\kappa_{vv}}{3\kappa^{5/3}} \approx \tilde{\mu} = \frac{\phi_{xx}\phi_{yy} - \phi_{xy}^2}{(\phi_{xx}\phi_y^2 - 2\phi_x\phi_{xy}\phi_y + \phi_x^2\phi_{yy})^{2/3}}.$$

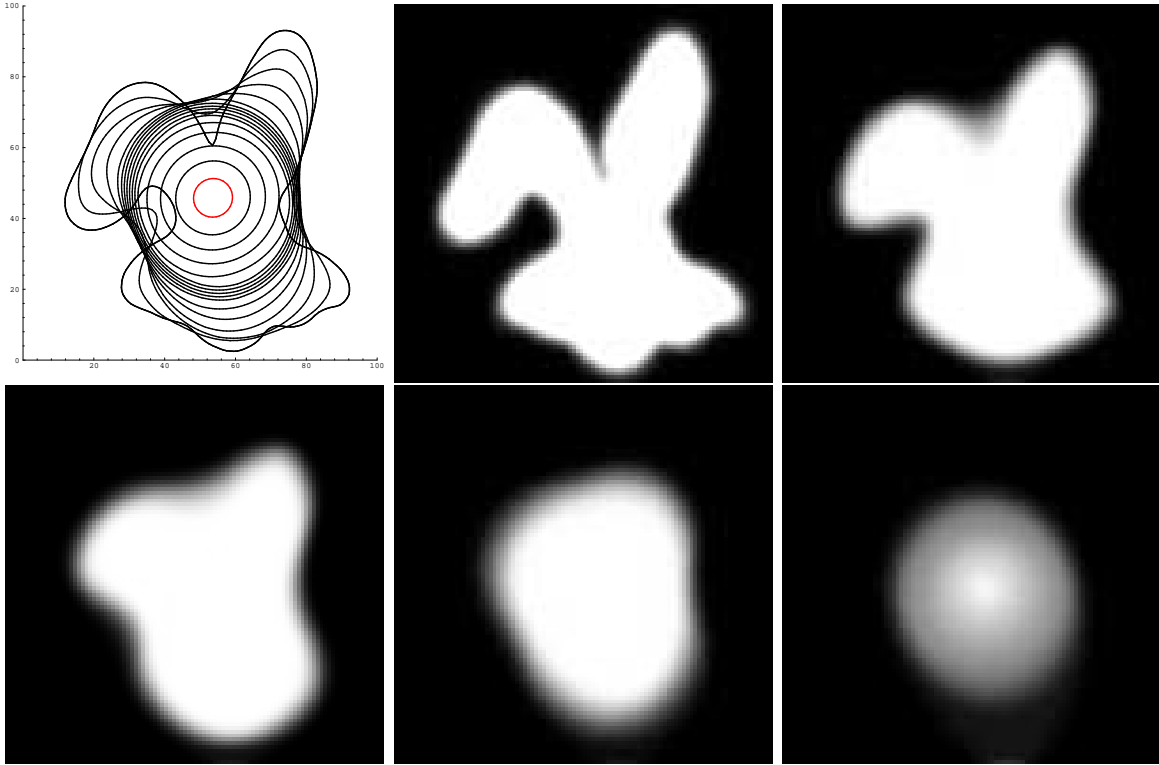


Figure 4: Affine curve evolution  $\mathcal{C}_t = \kappa^{1/3} \vec{\mathcal{N}}$  (zero sets), and 5 steps of the implicit evolution  $\phi_t = (\phi_y^2 \phi_{xx} - 2\phi_x \phi_y \phi_{xy} + \phi_x^2 \phi_{yy})^{1/3}$ , starting at the upper middle and ending at the lower right frame.



Figure 5: Affine invariant procedure for locating the convex hull of a shape: Evolution according to the weighted equi-affine geometric heat equation:  $\mathcal{C}_t = \frac{\kappa^{1/3}}{g^2} \vec{\mathcal{N}}$ , and four steps of the implicit implementation evolution,  $\phi(t)$  at  $t = 0, t_1, t_2, \infty$ . The edge enhancer  $g(x, y) = |G(\Delta T) \circ I(x, y)|$ , is affine invariant, so that the final result as well as every step along the evolution is invariant (under the equi-affine transformation)

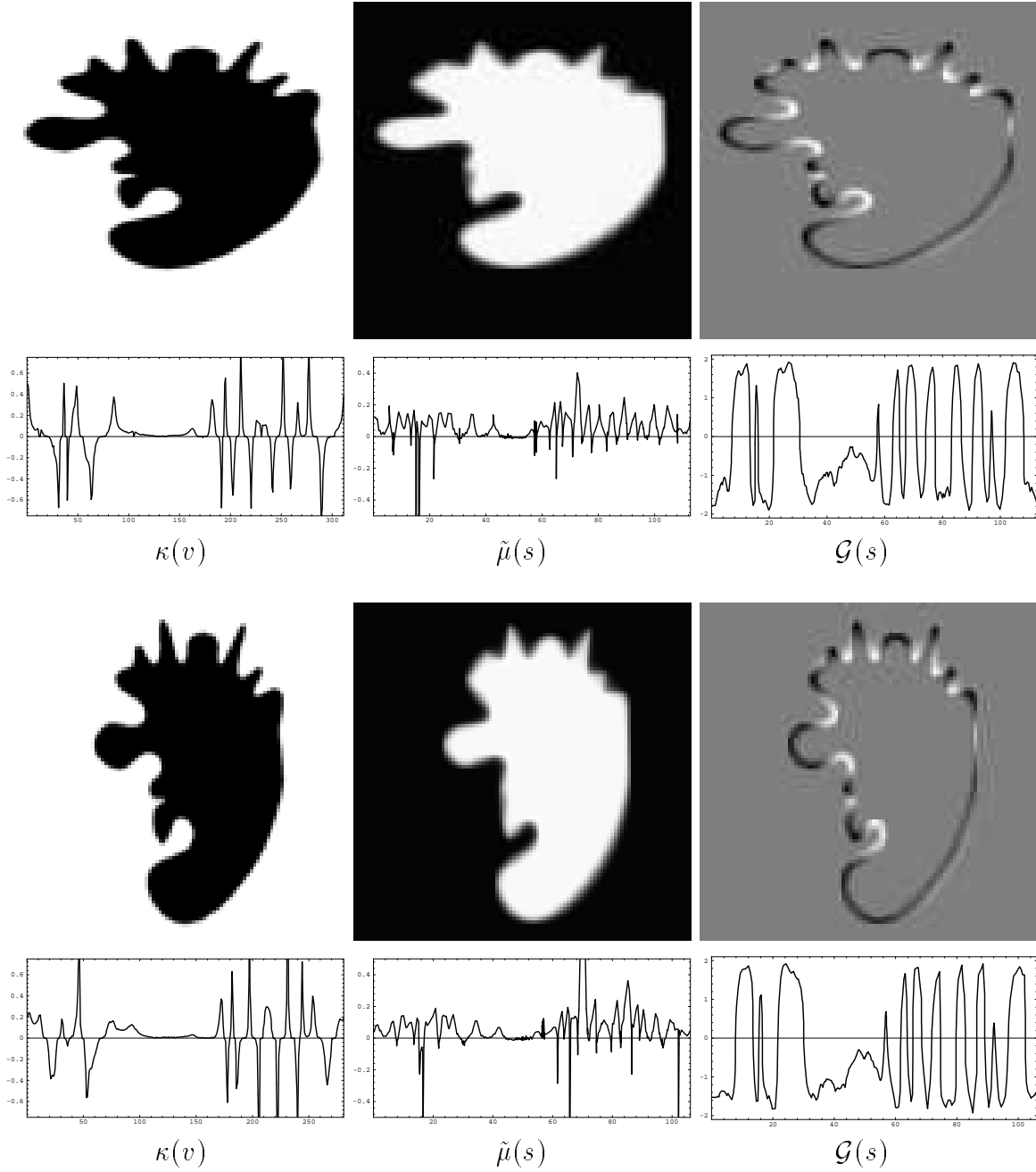


Figure 6: Invariant signatures under affine transformation: On the second and forth rows, from left to right are  $\kappa(v)$ ,  $\mu(s)$  and  $G(\Delta T) \circ I(x, y)$  samples along the zero level set (as a function of the affine arclength):  $\mathcal{G}(s)$ . On the first and third rows, from left to right are the shapes  $I(x, y)$ ,  $\phi(\Delta T)$ , and  $G(\Delta T) \circ I(x, y)$  respectively.

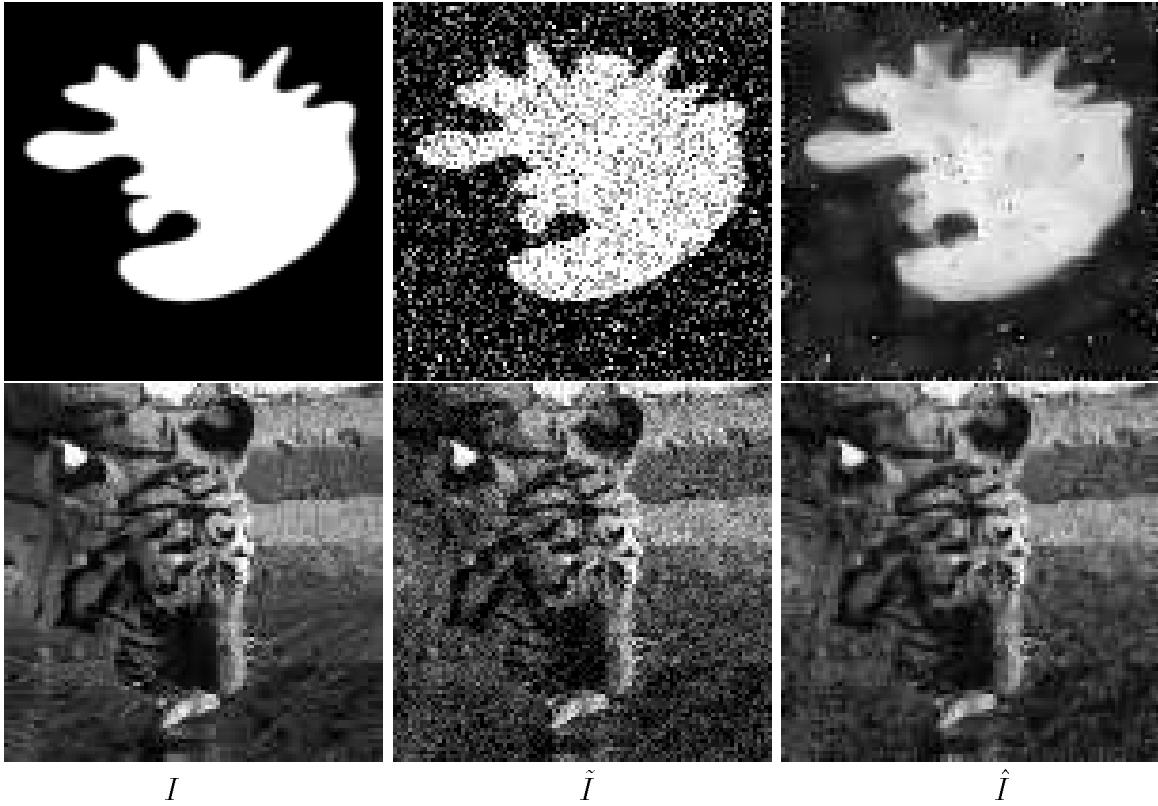


Figure 7: Image denoising algorithm results based on the weighted affine heat equation: From left to right: The original image  $I$ , the noisy image  $\tilde{I} = I + n$ , and the image after denoising  $\hat{I}$ . The noise was selected to be a Gaussian white noise, with  $SNR = 9$  for the face and  $SNR = 15$  for the tiger image. The results for the tiger are obtained after 12 iterations with  $dt = 0.005$ , and 4 smoothing iterations (performed every two iterations) for the computation of the edge enhancer with  $\Delta T = 0.05$ . For the face we have chosen 120 main iterations and 6 iterations for the enhancer (every two main iterations).

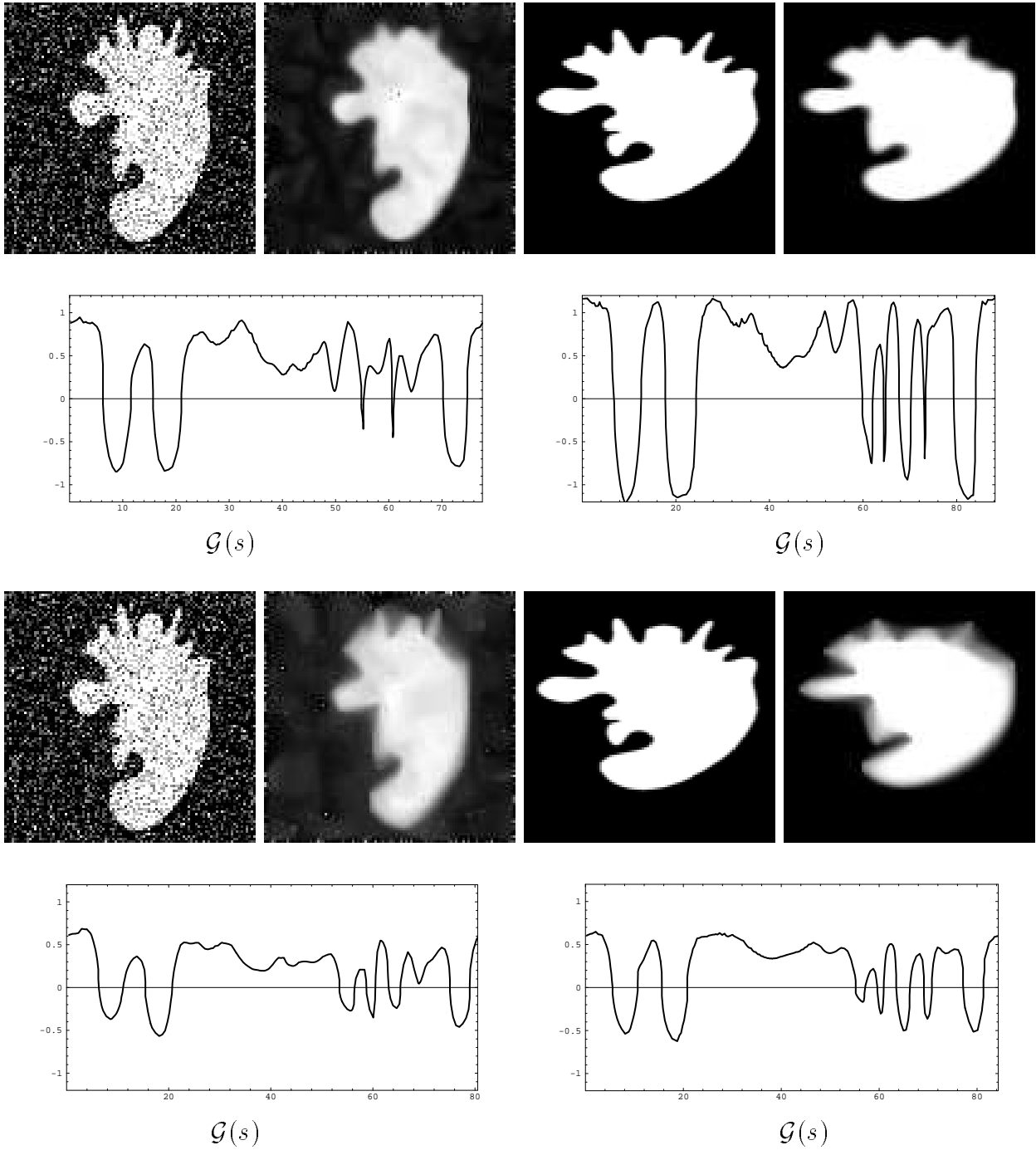


Figure 8: The smoothing invariant effect on the signature  $\mathcal{G}(s)$ . The two upper rows present the signatures obtained after smoothing with the Rudin-Osher-Fatemi algorithm. The lower rows present the signature after smoothing with the affine invariant selective smoothing procedures. Observe that the invariant smoothing better preserves the relation between the signatures.

## References

- [1] D Adalsteinsson and J A Sethian. A fast level set method for propagating interfaces. *J. of Comp. Phys.*, 118:269–277, 1995.
- [2] L Alvarez, F Guichard, P L Lions, and J M Morel. Axioms and fundamental equations of image processing. *Arch. Rational Mechanics*, 123, 1993.
- [3] L Alvarez, P L Lions, and J M Morel. Image selective smoothing and edge detection by nonlinear diffusion. *SIAM J. Numer. Anal.*, 29:845–866, 1992.
- [4] C Ballester. *An affine invariant model for image segmentation: Mathematical analysis and applications*. Ph.D. thesis, Univ. Illes Balears, Palma de Mallorca, Spain, March 1995.
- [5] C Ballester, V Caselles, and M Gonzalez. Affine invariant segmentation by variational method. Internal report, Univ. Illes Balears, Palma de Mallorca, Spain, 1995.
- [6] A M Bruckstein, R J Holt, A Netravali, and T J Richardson. Invariant signatures for planar shape recognition under partial occlusion. *CVGIP: Image Understanding.*, 58(1):49–65, 1993.
- [7] A M Bruckstein, N Katzir, M Lindenbaum, and M Porat. Similarity invariant recognition of partially occluded planar curves and shapes. *International Journal of Computer Vision*, 7:271–285, 1992.
- [8] A M Bruckstein and A Netravali. On differential invariants of planar curves and recognizing partially occluded planar shapes. AT&T technical report, AT&T, 1990.
- [9] A M Bruckstein, E Rivlin, and I Weiss. Scale space local invariants. Center for intelligent systems report, Technion–Israel Institute of Technology, Israel, 1995.
- [10] A M Bruckstein and D Shaked. On projective invariant smoothing and evolutions of planar curves and polygons. Center for Intelligent Systems Report CIS #9328, Technion–Israel Institute of Technology, Israel, November 1993.
- [11] Su Buchin. *Affine Differential Geometry*. Science Press, Beijing, China, 1983.
- [12] E Calabi, P J Olver, and A Tannenbaum. Affine geometry, curve flows, and invariant numerical approximations. Research report - the geometry center, University of Minnesota, June 1995.
- [13] J Canny. A computational approach to edge detection. *IEEE Trans. on PAMI*, 8(6):679–698, 1986.
- [14] V Caselles, R Kimmel, and G Sapiro. Geodesic active contours. In *Proceedings ICCV'95*, pages 694–699, Boston, Massachusetts, June 1995.

- [15] D L Chopp and J A Sethian. Flow under mean curvature: Singularity formation and minimal surfaces. Center for pure applied math. pam-541, Univ. of CA. Berkeley, November 1991.
- [16] T Cohignac, L Lopez, and J M Morel. Integral and local affine invariant parameters and application to shape recognition. In D Dori and A Bruckstein, editors, *Shape Structure and Pattern Recognition*. World Scientific Publishing, 1995.
- [17] C L Epstein and M Gage. The curve shortening flow. In A Chorin and A Majda, editors, *Wave Motion: Theory, Modeling, and Computation*. Springer-Verlag, New York, 1987.
- [18] L C Evans and J Spruck. Motion of level sets by mean curvature, I. *J. Diff. Geom.*, 33, 1991.
- [19] Olivier Faugeras and Renaud Keriven. Scale-space and affine curvature. In *Proceedings Europe-China Workshp on Geometrical modelling and Invariants for Computer Vision*, pages 17–24, 1995.
- [20] L M J Florack, B M ter Haar Romeny, J J Koenderink, and M A Vierever. General intensity transformations and differential invariants. *Journal of Mathematical Imaging and Vision*, 4:171–187, 1994.
- [21] M Gage and R S Hamilton. The heat equation shrinking convex plane curves. *J. Diff. Geom.*, 23, 1986.
- [22] I M Gelfand and S V Fomin. *Calulus of variations*. Prentice-Hall, Inc., Englewood Cliffs, New Jersey, 1963.
- [23] R Kimmel and A M Bruckstein. Shape offsets via level sets. *CAD*, 25(5):154–162, March 1993.
- [24] T Lindeberg and B M ter Haar Romeny. Linear scale-space II: Early visual operations. In B M ter Haar Rommeny, editor, *Geometric-Driven Diffusion in Computer Vision*. Kluwer Academic Publishers, The Netherlands, 1994.
- [25] R Malladi, J A Sethian, and B C Vemuri. Shape modeling with front propagation: A level set approach. *IEEE Trans. on PAMI*, 17:158–175, 1995.
- [26] T Moons, E J Pauwels, L J Van Gool, and A Oosterlinck. Foundations of semi-differential invariants. *Int. J. of Computer Vision*, 14(1):49–65, 1995.
- [27] P J Olver, G Sapiro, and A Tannenbaum. Invariant geometric evolutions of surfaces and volumetric smoothing. MIT report - LIDS, MIT, April 1994.
- [28] P J Olver, G Sapiro, and A Tannenbaum. Affine invariant edge maps and active contours. Research report - the geometry center, University of Minnesota, October 1995.
- [29] Peter J Olver. *Equivalence, Invariants, and Symetry*. Cambridge University Press, Cambridge-UK, 1995.

- [30] S J Osher and L I Rudin. Feature-oriented image enhancement using shock filters. *SIAM J. Numer. Analy.*, 27(4):919–940, August 1990.
- [31] S J Osher and J A Sethian. Fronts propagating with curvature dependent speed: Algorithms based on Hamilton-Jacobi formulations. *J. of Comp. Phys.*, 79:12–49, 1988.
- [32] P Perona and J Malik. Scale-space and edge detection using anisotropic diffusion. *IEEE-PAMI*, 12:629–639, 1990.
- [33] L Rudin, S Osher, and E Fatemi. Nonlinear total variation based noise removal algorithms. *Physica D*, 60:259–268, 1992.
- [34] G Sapiro. *Topics in Shape Evolution*. D.Sc. thesis (in Hebrew), Technion - Israel Institute of Technology, April 1993.
- [35] G Sapiro and A Tannenbaum. Affine invariant scale-space. *International Journal of Computer Vision*, 11(1):25–44, 1993.
- [36] G Sapiro and A Tannenbaum. On invariant curve evolution and image analysis. *Indiana University Mathematics Journal*, 42(3), 1993.
- [37] G Sapiro and A Tannenbaum. On affine plane curve evolution. *Journal of Functional Analysis*, 119(1), 1994.
- [38] G Sapiro, A Tannenbaum, Y L You, and M Kaveh. Experimenting on geometric image enhancement. In *Proceedings IEEE ICIP*, volume 2, pages 472–476, Austin, Texas, November 1994.
- [39] M Sussman, P Smereka, and S J Osher. A level set approach for computing solutions to incompressible two-phase flow. *J. of Computational Physics*, 114:146–159, 1994.